



## Design a full-scale batch adsorber for separation of thorium(IV) from liquid effluents by *Haloxylon persicum* leaves

Mohamed Ahmed Mahmoud

Chemical Engineering Department, College of Engineering, Jazan University, Jazan, Saudi Arabia, Tel. +966564442596; email: Momahmoud@jazanu.edu.sa

Received 17 December 2020; Accepted 6 May 2021

---

### ABSTRACT

*Haloxylon persicum* leaves were used as adsorbent biomass in the separation of thorium ions from an aqueous batch system. *H. persicum* leaves were characterized by Fourier transform infrared spectroscopy, energy-dispersive X-ray spectroscopy, X-ray diffraction, and Brunauer–Emmett–Teller analyses. The maximum separation (99.78%) and sorption capacity (18.82 mg/g) were obtained at 0.3 g *H. persicum* leaves dose, pH 5, 60 min, 100 mg Th(IV), and 30°C. The experimental outputs were modeled by the nonlinear method to examine appropriate isotherm and kinetic sorption in the exothermic batch system. The results appeared that the Langmuir and pseudo-second-order were the best fitting models. Also, *H. persicum* leaves has can be used in the adsorption-desorption system for up to seven cycles. The sorption system was scaled up to design a full-scale sorption system using the best fitting isotherm (Langmuir). The results indicated that the *H. persicum* leaves could be used as eco-friendly and low-cost biodegradable biomass for the effective sorption of Th(IV) from the aqueous system in pilot and full-scale systems.

*Keywords:* Sorption; Th(IV); *Haloxylon persicum*; Kinetics; Thermodynamic

---

### 1. Introduction

Energy demand has increased in recent years as a result of economic development, which has led to the search for new sources of energy other than conventional sources. Energy derived from nuclear applications is one of the alternative energy sources [1,2]. The trend toward energy production from nuclear applications has reduced dependence on conventional fuels, and thus the environmental pollution emitted from them [3,4]. However, nuclear applications produce pollutants of a more dangerous nature and need to be treated more than the waste produced from conventional fuel pollutants [5]. The development helped in establishing different types of nuclear power plants to supply countries with the energy needed

for various fields such as electricity production and others, but it increased the amount of waste that is more dangerous than the waste of conventional fuels [6,7]. The great risk of residues resulting from nuclear applications lies in the radioactivity that results from them, which poses a great danger to human tissues, such as vital tissue damage and also cancer [8,9]. Uranium element is the main component in the manufacture of nuclear fuel, but due to the great pollution of radioactive waste and the cost of disposal, therefore, there is a tendency to use thorium as an alternative fuel to reduce the many years of continuous radioactive pollution that uranium causes to the environment [10]. Thorium is the second element in the manufacture of nuclear fuel and also has other uses such as the preparation of catalysts, high-temperature ceramic, and lenses [11].

There are many treatment processes for high concentrations radioactive liquid waste such as membranes [12], extraction [13], chemical precipitation [14], adsorption [15–18], and evaporation [19]. At low concentrations of radioactive contaminants, the adsorption process is effective and less costly than other processes whether in the materials used or in the operation [20]. Many adsorbent materials were used in the adsorption process such as chitosan resin [21], magnetic talc titanium oxide composite [22], water hyacinth roots [23], monetite [24], natural sepiolite [25], modified mesoporous silica SBA-15 [26], mesoporous solid materials [27], and hydroxyapatite microspheres [28], but natural materials are distinguished by their ability to decompose naturally (biodegradable materials), making them environmentally friendly [20]. In this research, a natural adsorbent material was selected that is characterized by its ability to decompose naturally (biodegradable materials), making it environmentally friendly. *Haloxylon persicum* is a desert plant, available in Arab countries, and it tolerates high temperature and salinity. It is used in the treatment of bone pain and burns. *H. persicum* leaves were used as an eco-friendly and low-cost biodegradable biomass for the effective sorption of Th(IV) from the aqueous system in a batch pilot system and also, for the design of a full-scale system. Sorption conditions such as pH, sorbent dose, inlet thorium concentration, adsorption time, and temperature were investigated. The sorption isotherms, kinetics, and thermodynamics were studied. Also, the economic feasibility of *H. persicum* leaves was studied by the sorption-desorption system.

## 2. Materials and methods

### 2.1. Chemicals

Analytical grade of chemicals and reagents obtained from Sigma Aldrich Company was used in the work. Thorium nitrate  $\text{Th}(\text{NO}_3)_4$  was utilized in the preparation of feedstock solution with distilled water, and the adjustment of pH was implemented by HCl and NaOH.

### 2.2. Preparation of biosorbent

*H. persicum* leaves were obtained from the local herbal market. *H. persicum* leaves were cut into 0.5 cm pieces and washed with distilled water to remove foreign substances. Then, *H. persicum* leaves were dried at 80°C until fixed weight and then ground into 75 mesh.

### 2.3. Adsorption procedure

The optimum sorption parameters were determined in the batch procedure by change one parameter and fixed other parameters. The batch experimental procedure was achieved in a 200 mL glass flask by added 0.5 g of *H. persicum* leaves to 100 mL of Th(IV) ion with stirring at 200 rpm in a thermostatic shaker water bath at 30°C (Julabo, Model SW -20°C, Germany). At equilibrium, *H. persicum* leaves were separated from samples by centrifugation at 5,000 rpm for 3 min then filtered. The samples were analyzed by spectrophotometric procedure by arsenazo(III) using Shimadzu

UV-VIS-1601 spectrophotometer at 665 nm [25]. The removal percent  $P_R$  (%) of Th(IV) and maximum adsorption capacity  $q_e$  (mg/g) were calculated by the following equations:

$$P_R (\%) = \frac{\text{Inlet concentration} - \text{Final concentration}}{\text{Inlet concentration}} \times 100 \quad (1)$$

$$q_e = \frac{(\text{Inlet concentration} - \text{Final concentration}) \times (\text{Operating volume})}{\text{Dose of biomass}} \quad (2)$$

### 2.4. Sorption isotherm studies

Sorption isotherm of thorium uptake onto *H. persicum* leaves was studied by Freundlich, Langmuir, and Redlich–Peterson isotherms by the nonlinear system. The relative standard deviations of optimum sorption isotherm were determined using error functions (Marquardt's percent standard deviation (MPSD), and Chi-square ( $\chi^2$ )) [9,23].

$$\chi^2 = \sum_{i=1}^n \frac{\sum_{i=1}^n (q_{e,\text{experimental}} - q_{e,\text{theoretical}})^2}{q_{e,\text{theoretical}}} \quad (3)$$

$$\text{MPSD} = \sum_{i=1}^n \left[ \frac{q_{e,\text{experimental}} - q_{e,\text{theoretical}}}{q_{e,\text{theoretical}}} \right]^2 \quad (4)$$

#### 2.4.1. Langmuir model

Langmuir isotherm is utilized to describe the monolayer sorption of Th(IV) onto *H. persicum* leaves and is expressed by the equation [29]:

$$q_e = \frac{Q_L K_L C_f}{(1 + K_L C_f)} \quad (5)$$

where  $C_f$  is the equilibrium Th(IV) concentration (mg/L).  $Q_L$  (mg/g) and  $K_L$  (L/mg) are the Langmuir constants.

#### 2.4.2. Freundlich model

Freundlich isotherm [30] regulates the strength of Th(IV) attraction on the *H. persicum* leaves by Eq. (6):

$$q_e = K_F C_f^{1/n} \quad (6)$$

where  $K_F$  ( $\text{mg}^{(1-1/n)} \text{L}^{1/n} \text{g}^{-1}$ ) is the Freundlich constant and  $n$  is a parameter that denotes the strength Th(IV) attraction onto *H. persicum* leaves.

#### 2.4.3. Redlich–Peterson model

Redlich–Peterson isotherm was used to describe the homogenous or heterogeneous sorption processes and definite by the following equation [9]:

$$q_e = K_{RP} C_f \left( 1 + F C_f^{\beta} \right) \quad (7)$$

where  $K_{RP}$  (L/g) and  $F$  (L/mg)<sup>β</sup> are Redlich–Peterson constants and the item of β is an exponent referred to as the energy of Th(IV) binding with the *H. persicum* leaves.

### 2.5. Sorption kinetic studies

Non-linear methods were used to evaluate the sorption kinetics using pseudo-first-order, pseudo-second-order, and Elovich kinetic models.

#### 2.5.1. Pseudo-first-order model

This model assumes that the physisorption is the controlling in Th(IV) binding with the *H. persicum* leaves [9], and is described by the subsequent equation:

$$q_t = q_e (1 - e^{-K_1 t}) \quad (8)$$

where  $q_e$  and  $q_t$  are the sorption capacity at equilibrium and any time  $t$  (mg/g) and the symbol  $K_1$  (L/min) and  $K_2$  (g/mg min) are the pseudo-first-order and the pseudo-second-order kinetic model constants, respectively.

#### 2.5.2. Pseudo-second-order model

The model assumed that the physicochemical behavior is the main cause of sorption and is explained by Eq. (9) [31]:

$$q_t = \frac{K_2 q_e^2 t}{1 + K_2 q_e t} \quad (9)$$

where  $K_2$  (g/mg min) is the pseudo-second-order kinetic model constants.

#### 2.5.3. Elovich kinetic model

The Elovich equation is used to describe the chemisorption process supposing that the biomass surfaces are dynamically heterogeneous and is described by Eq. (10) [32,33]:

$$\frac{dq_t}{dt} = \alpha \exp(-\beta dt) \quad (10)$$

where  $\alpha$  is a parameter that refers to sorption rate (mg/g min) and  $\beta$  refers to the uptake of biomass (mg/g).

## 3. Results and discussion

### 3.1. Characterization

#### 3.1.1. Brunauer–Emmett–Teller analysis

The Brunauer–Emmett–Teller (BET) surface area of *H. persicum* leaves before sorption was 2.5561 m<sup>2</sup>/g, but after Th(IV) uptake was decreased to 1.2453 m<sup>2</sup>/g due to Th(IV) ion interaction with *H. persicum* leaves surface (Fig. 1).

#### 3.1.2. X-ray diffraction analysis

The X-ray diffraction (XRD) examinations of *H. persicum* leaves before and after Th(IV) uptake are shown in

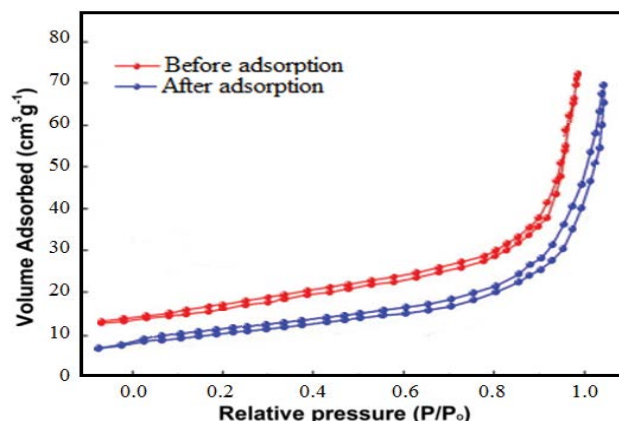


Fig. 1. BET analysis before and after of Th(IV) adsorption onto *Haloxylon persicum* leaves.

Fig. 2a. Before Th(IV) sorption, the XRD pattern of *H. persicum* leaves have three diffraction peaks at  $2\theta = 14.81^\circ$ ,  $20.94^\circ$ , and  $28.99^\circ$  referring to the crystalline structure, whereas after Th(IV) sorption, the peaks at  $2\theta = 14.81^\circ$  and  $20.94^\circ$  became less intensity and the peak at  $2\theta = 28.99^\circ$  disappeared. Furthermore, new peaks at  $2\theta = 46.59^\circ$  and  $66.67^\circ$  were appeared due to the sorption of thorium ions on the *H. persicum* leaves. These changes led to a small decreasing in the crystal structure of the biomass as a result of the sorption process [30].

#### 3.1.3. Fourier transformed infrared spectroscopy analysis

Fourier transformed infrared spectroscopy (FT-IR) analysis demonstrates the surface properties and the existence of different functional groups (active sites) in the *H. persicum* leaves which determine the interactions with Th(IV) ions and hence supportive to explain the sorption mechanism [29]. FT-IR spectrum before and after Th(IV) sorption (Fig. 2b) and listed in Table 1. The FT-IR spectrum after Th(IV) sorption indicates that no alteration in the FT-IR spectrum of *H. persicum* leaves, but a small shift in the wavelength with the reduction in the transmittance of some peaks has appeared. These decreasing in the intensity with small shifts in the peak wavelengths of functional O–H, C–H, and C=O groups demonstrate the sorption mechanism of thorium ions onto *H. persicum* leaves along with the subsequent stages (a) Th<sup>4+</sup> moves to the *H. persicum* leaves surface in the sorption system, (b) electrostatic attraction of Th<sup>4+</sup> with charges of *H. persicum* leaves active sites, (c) Th<sup>4+</sup> interconnected with the *H. persicum* leaves functional groups. This suggesting the complexation and/or ion exchange interaction between Th<sup>4+</sup> and active sites of *H. persicum* leaves functional groups [9,30].

#### 3.1.4. Energy-dispersive X-ray spectroscopy investigation

The energy-dispersive X-ray (EDS) analysis is a technique used to identify the constituent elements of adsorbent. This technique is important because it confirms the ability of the adsorbent material to adsorb the elements by comparing the analysis of the adsorbent material before

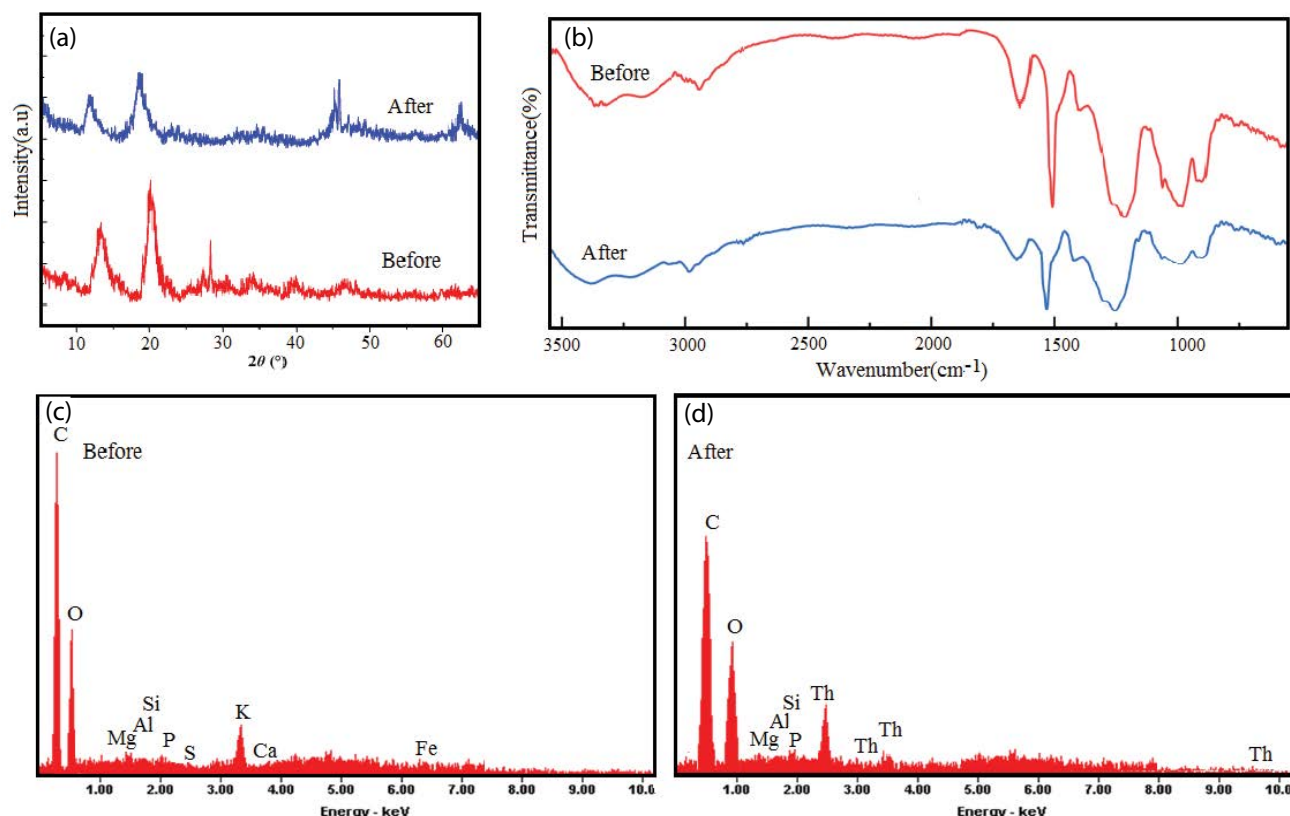


Fig. 2. XRD (a), FTIR (b), and EDS (c) analysis before and after of Th(IV) adsorption onto *Haloxylon persicum* leaves.

Table 1  
FTIR analysis of *Haloxylon persicum* leaves before and after Th(IV) sorption

Peak wavelength (cm <sup>-1</sup> )		Assignment
Before sorption	After sorption	
3,455	3,445	O–H stretching vibrations of hydroxyl groups
2,899	2,909	C–H asymmetric stretching vibration of the methyl group
1,770	1,766	C=O stretch of COOH
1,622	1,634	C=O of amide
1,530	1,510	Aromatic C=C stretching and/or asymmetric C–O stretch in COO-in aromatics
1,477	1,451	C–O stretching vibrations
1,250	1,233	C–O stretching of phenolic OH
1,122	1,120	Aromatic C=C stretching Lignin
1,021	1,011	C–O stretching vibrations
855	831	Aromatic CH

and after the adsorption [30,31]. The EDS analysis before and after Th(IV) uptake onto *H. persicum* leaves is showed in Fig. 2c and d. The XRD analysis of *H. persicum* leaves before adsorption (Fig. 2c) shows that the elements of K, C, O, Fe, Mg, P, S, and Ca are the chief elements of *H. persicum* leaves whereas, the EDS analysis after Th(IV) sorption (Fig. 2d) shows the appearance of Th(IV) ions around 2.7, 3.1, 3.5, and 9.8 keV. These outcomes assured the adsorption of thorium ions onto active sites of *H. persicum* leaves.

### 3.2. Sorption dynamic studies

The pH of the inlet sorption solution is an essential factor controlling the interaction of Th(IV) ions onto active sites of *H. persicum* leaves. Th(IV) sorption onto *H. persicum* leaves was investigated in the pH range (2–8) using 0.5 g *H. persicum* leaves and 10 mg/L of Th(IV) at 30°C with interval time (10–100 min) (Fig. 3a). The outcomes show that the maximum Th(IV) removal (99.78%) was increased up to pH 5 then decreased with elevated pH after 5.

The increases of  $P_R$  (%) with pH increase (from 2 to 5) owing to the decreasing of the competition between Th(IV) ions and  $H^+$  on the active points of *H. persicum* leaves, but, the reduction in  $P_R$  (%) with elevated pH owing to the formation of insoluble Th(IV) compounds by precipitation effect[29]. Also, the experimental results (Fig. 3a) show the maximum Th(IV) removal was obtained at an equilibrium sorption time of 60 min. The equilibrium *H. persicum* leaves dose was studied in the dose range (0.1–0.7 g) at conditions (10 mg/L Th(IV), 60 min, 30°C, and pH 5). Fig. 3b shows an upturn in the  $P_R$  (%) with increasing of *H. persicum* leaves dose consequently of an increase of energetic sorption sites [9]. The equilibrium  $P_R$  (%) was reached at 0.3 g, then no noteworthy change with dose upturn whether adsorption capacity was decreased with increasing *H. persicum* leaves dose [29]. The effect of Th(IV) feed concentration was examined in the range of (10–40 mg/L) at 0.3 mg dose, 60 min, 30°C, and pH 5 (Fig. 3c) display that the  $P_R$  (%) was declined from 99.78% to 46.56% with the rising of Th(IV) feed concentration from 10 to 40 mg/L, however, the Th(IV) uptake increases from 9.77 to 18.82 mg/g owing to the growing of Th(IV) on the active sites of *H. persicum* leaves [25].

The temperature range of (30°C–45°C) was utilized in the examination of the heating effect in the Th(IV) removal at 0.3 mg dose, 60 min, 40 mg/L Th(IV), and pH 5. Fig. 3d indicates that the  $P_R$  (%) of Th(IV) decreases slowly with increasing the temperature from 30°C to 45°C, due to the reversible interaction between Th(IV) and active sorption sites with the temperature rise which confirmed the exothermic nature of the Th(IV) uptake onto *H. persicum* leaves [23].

3.3. Competitive uptake of metal ions

The sorption capacity of Th(IV) ions by *H. persicum* leaves was studied in the presence of other metal ions such as cadmium, iron, uranium, and zinc ions in the adsorption systems (40 mg/L Th/15 mg/L of other metal ions) to indicate the sorption selectivity of *H. persicum* leaves under the optimum operating conditions. Fig. 4 shows that the adsorption capacity of *H. persicum* leaves for Th(IV) ions in the single sorption system was higher than the obtained with the mixed sorption system. This is maybe owing to the difference in the electrostatic attraction force between metal ions and the negative charge of adsorption

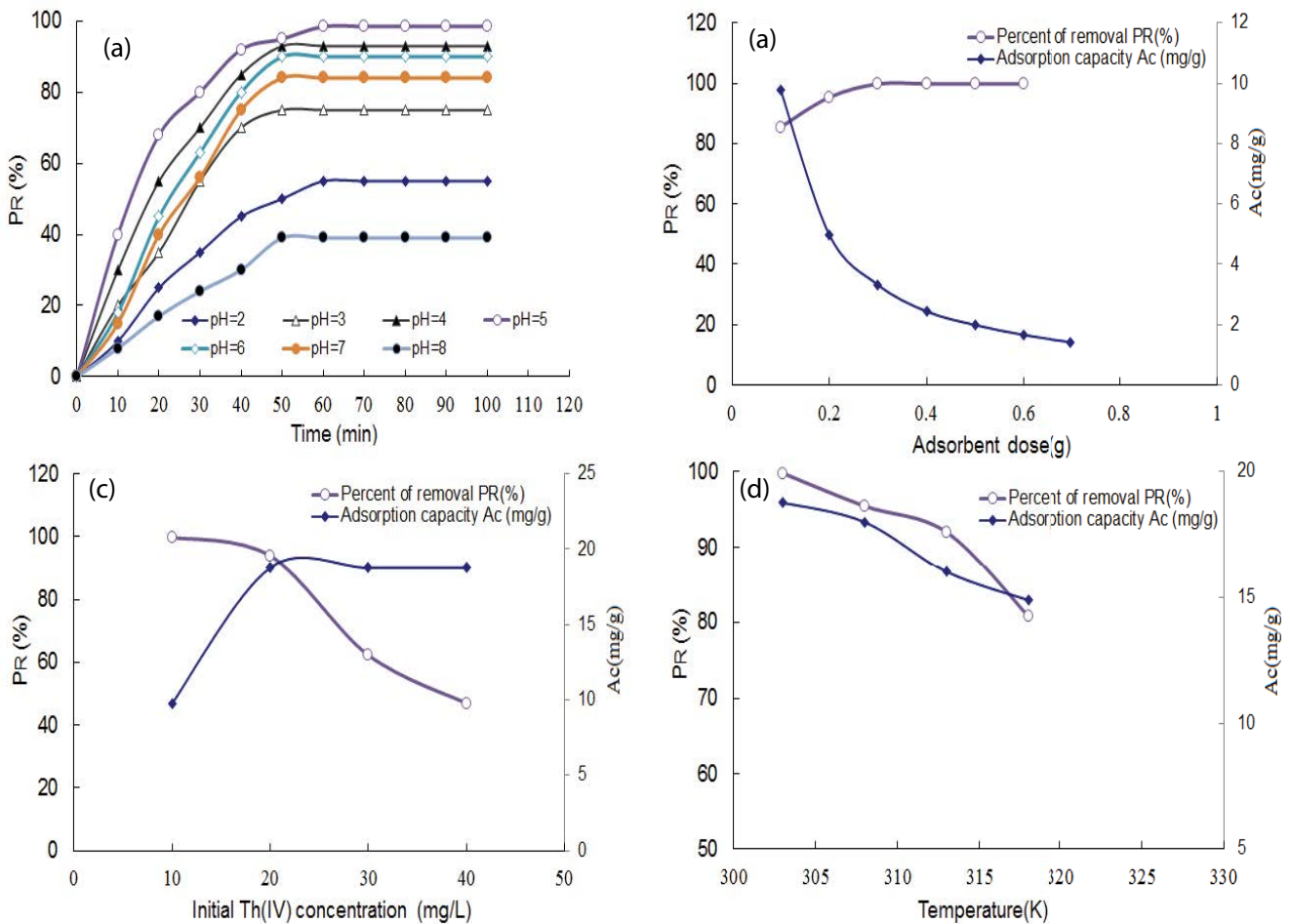


Fig. 3. Sorption dynamic studies of Th(IV) onto *Haloxylon persicum* leaves (a) pH effect: condition (0.5 g dose and 10 mg/L Th(IV) and 30°C), (b) dose effect: condition (10 mg/L Th(IV), 60 min, 30°C, and pH 5), (c) initial concentration effect: condition (0.3 mg dose, 60 min, 30°C, and pH 5), temperature effect: condition (0.3 mg dose, 60 min, 20 mg/L Th(IV), and pH 5).

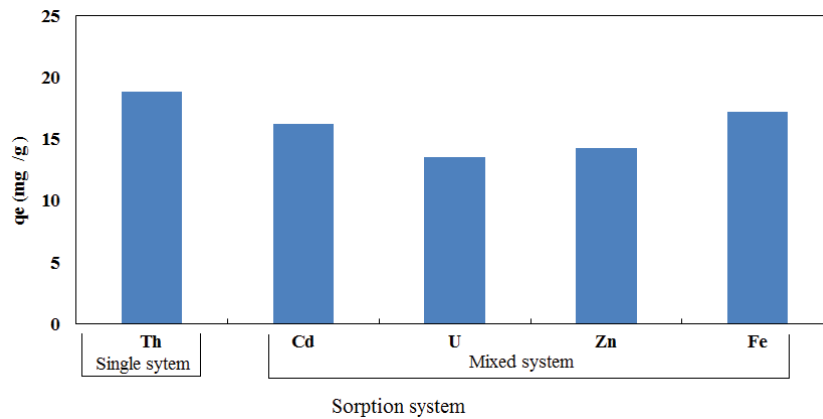


Fig. 4. Competitive uptake of metal ions at conditions (40 mg/L Th/15 mg/L of other metal ions, 0.3 mg dose, 60 min, 30°C, and pH 5).

sites of *H. persicum* leaves, which is associated with the ionic hydration of the studied metal ions [33].

### 3.3.1. Sorption isotherm modeling

Fig. 5a shows the plots of nonlinear isotherm models and the constants of isotherms are listed in Table 2. The results indicate that the sorption data has well-fitting with the Langmuir isotherm owing to the higher correlation coefficient ( $R^2$ ) and lower chi-square analysis ( $\chi^2$ ) and MPSD than other models. This result suggesting that monolayer sorption of Th(IV) ions onto the *H. persicum* leaves surface [31]. The agreement between experimental (18.82 mg/g) and calculated adsorption capacity (19.125) also confirms these results.

### 3.3.2. Sorption kinetic modeling

The nonlinear plots of kinetic models (Fig. 5b) and the results of kinetic parameters (Table 2) show a good convergence between calculated (18.82 mg/g) and trial

(18.95 mg/g) adsorption capacity with a pseudo-second-order model. Also, the higher value of the correlation coefficient ( $R^2$ ) and lower values of  $\chi^2$  and MPSD confirmed that the pseudo-second-order model was the best fitting model for the sorption of Th(IV) ions onto *H. persicum* leaves. While both pseudo-first-order and Elovich kinetic models did not give results consistent with the outcomes of sorption.

### 3.4. Design of full-scale batch unit

The full-scale batch unit was designed by a mass balance between the inlet and outlet sorption parameters using the best fitting adsorption isotherm (Langmuir) to determine the *H. persicum* leaves dose required to treat a known volume of Th(IV) waste liquid which is the essential parameters to design a full-scale batch unit [34]. Fig. 6a shows a process flow diagram of the batch sorption unit. Mathematical equations of the following items were used to determine the optimum amount of *H. persicum* leaves dose  $M$  (g) required to treat the volume of feed liquid  $V_f$  ( $m^3$ ) from initial Th(IV) concentration  $C_i$  (mg/L)

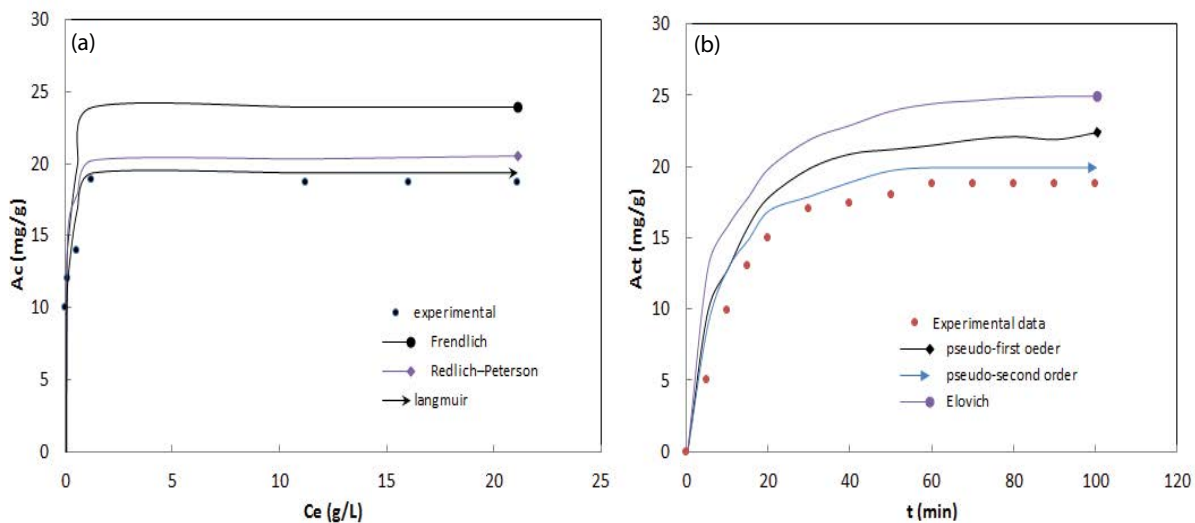


Fig. 5. Nonlinear sorption (a) isotherm (0.3 mg dose, 60 min, and pH 5) and (b) kinetic (0.3 mg dose, 20 mg/L Th(IV), and pH 5) models of Th(IV) onto *Haloxylon persicum* leaves.

Table 2  
Nonlinear kinetic and isotherm models parameters of Th(IV) sorption onto *Haloxylon persicum* leaves

Kinetic model	Experimental adsorption capacity (mg/g)	Parameter value	Isotherms	Parameter value
Pseudo-first-order	18.82		Langmuir	
$k_1$ (min <sup>-1</sup> )		0.3125	$K_L$ (L/mg)	9.2545
$q_e$ (mg/g)		38.585	$Q_L$ (mg/g)	19.125
$R^2$		0.8564	$R^2$	0.9910
$\chi^2$		2.2407	$\chi^2$	0.1187
MPSD		0.846	MPSD	0.0130
Pseudo-second-order			Freundlich	
$k_2$ (g/mg min)		0.0612	$K_f$ (mg <sup>(1-1/n)</sup> L <sup>1/n</sup> g <sup>-1</sup> )	33.896
$q_e$ (mg/g)		18.425	$n$	4.2410
$R^2$		0.9945	$R^2$	0.9612
$\chi^2$		0.2196	$\chi^2$	2.5039
MPSD		0.0131	MPSD	0.521
Elovich			Redlich–Peterson	
$\alpha$		5,864.5	$A_R$ (L/g)	1,124.1
$\beta$		1.9871	$B_R$ (L/mg) <sup><math>\beta</math></sup>	22.633
$R^2$		0.9425	$\beta$	0.5531
$\chi^2$		5.4212	$R^2$	0.9855
MPSD		0.597	$\chi^2$	0.3393
			MPSD	0.6631

to final Th(IV) concentration  $C_f$  (mg/L). The adsorption limit of *H. persicum* leaves was altered from  $q_i$  to  $q_e$ . Mass equilibrium of info and yield boundaries of full-scale adsorber unit was resolved as follows:

$$V_f(C_i - C_f) = M(q_i - q_e) \quad (11)$$

When  $q_i = 0$ :

$$V_f(C_i - C_f) = M(q_e) \quad (12)$$

$$\frac{M}{V_f} = \frac{(C_i - C_f)}{q_e} \quad (13)$$

From linear Langmuir isotherm:

$$q_e = \frac{Q_L K_L C_f}{(1 + K_L C_f)} \quad (14)$$

By replacing  $q_e$  in Eq. (15):

$$\frac{M}{V_f} = \frac{(C_i - C_f)(1 + K_L C_f)}{Q_L K_L C_f} \quad (15)$$

By substituting the values of Langmuir parameters  $Q_L$  and  $K_L$ , Eq. (15) becomes as follows:

$$M = V_f(C_i - C_f)(0.05229) \quad (16)$$

The *H. persicum* leaves dose required to treat a known volume of Th(IV) waste liquid from  $C_i$  (Th(IV) feed concentration) to  $C_f$  (Th(IV) final concentration) was regulated from Eq. (16). Fig. 6b shows the amount of *H. persicum* leaves dose required to treat a given volume of Th(IV) waste liquid or vice versa when applying on a full-scale system.

### 3.5. Thermodynamic studies

Thermodynamics dynamic (Enthalpy  $\Delta H$ , free energy  $\Delta G$ , and entropy  $\Delta S$ ) are determined from the slope and intercept of the equation (Van't Hoff) of the straight line obtained from subsequent equations [9,31].

$$\log K_D = \frac{\Delta S}{2.303R} - \frac{\Delta H}{2.303RT} \quad (17)$$

Also, free energy  $\Delta G$  was determined from the following equation:

$$\Delta G = \Delta H - T\Delta S \quad (18)$$

where  $T$  is the temperature (K),  $R$  is the gas constant (8.314 J/mol K):

$$K_D = \frac{A_c}{C_f} \quad (19)$$

where  $C_f$  and  $A_c$  are Th(IV) concentration (mg/L) and adsorption capacity (mg/g) at equilibrium, respectively.

Table 3 demonstrates that the negative values of free energy  $\Delta G$  decrease with the temperature rising, demonstrating that the spontaneous process of Th(IV) uptake onto

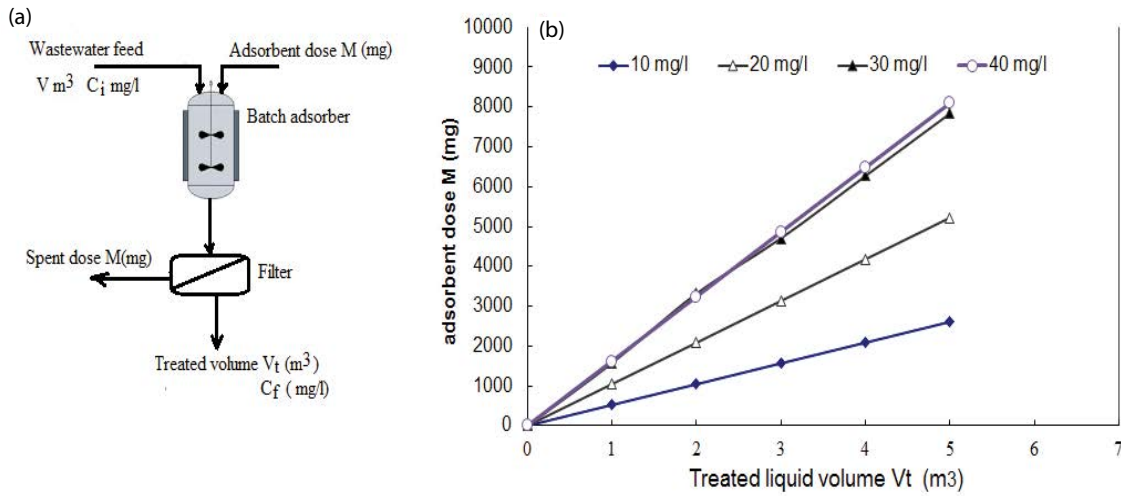


Fig. 6. Process flow diagram of batch adsorption unit (a) *Haloxylon persicum* leaves dose required to treat the different volumes of different Th(IV) feed concentrations (b).

Table 3  
Thermodynamic parameters of Th(IV) sorption onto *Haloxylon persicum* leaves

T (K)	lnK <sub>D</sub>	ΔG (kJ/mol)	ΔH (kJ/mol)	ΔS (kJ/mol k)
303	4.221	-251.04	-388.055	-0.452
308	3.054	-248.78		
313	2.320	-246.52		
318	0.876	-244.26		

*H. persicum* leaves. The value of enthalpy indicates the nature and type of the sorption process. The sorption system is exothermic when ΔH is a negative value while when ΔH is a positive value it is an endothermic [20].

Type of adsorption: 20–40 kJ/mol k = physisorption  
80 – 400 kJ/mol k = chemisorption

The negative ΔH (-388.055 kJ/mol) confirms the exothermic Th-*H. persicum* leaves sorption system. Also, the negative ΔS (-0.452 kJ/mol k) denotes the growth of randomness at the solid/solution interface [29].

### 3.6. Regeneration and recycling system

Biomass regeneration and metal recovery are the main economic reason for the desorption process [30]. Three eluting solutions (HNO<sub>3</sub>, HCl, and H<sub>2</sub>SO<sub>4</sub>) of different concentrations (1, 1.5, and 2 M) were used to run the desorption system. In a thermostatic water shaker bath for 1 h at 30°C 1.0 g of loaded *H. persicum* leaves was regenerated with 100 mL of eluting solutions. Table 4 displays that 1 M HNO<sub>3</sub> was the superlative eluting solution for desorption of Th(IV) ions into the solvable form than other eluting solutions. H<sup>+</sup>-Th<sup>4+</sup> substituting system is the basic mechanism of the desorption process [29]. Desorption percent was calculated by the subsequent equation:

Table 4  
Effect of eluting agents on Th(IV) desorption (%)

Eluting agent concentration	Desorption (%)		
	HNO <sub>3</sub>	HCl	H <sub>2</sub> SO <sub>4</sub>
0.5 M	92.41	88.39	82.46
1.0 M	98.45	91.75	87.47
1.5 M	98.44	92.10	88.48
2.0 M	98.45	92.22	89.88

Table 5  
Sorption–desorption cycles of on Th(IV) desorption (%) by *Haloxylon persicum* leaves

No. of cycle	Adsorption (%)
1	98.782
2	98.012
3	95.120
4	88.421
5	81.652
6	66.417
7	51.450
8	41.782
9	33.421
10	22.421

$$\text{Desorption}(\%) = \frac{\text{Desorption Th(IV) ions}}{\text{Adsorption Th(IV) ions}} \times 100 \quad (20)$$

From Table 5, it is obvious that *H. persicum* leaves were found to be used up to 7 cycles of the sorption–desorption system before the P<sub>R</sub> (%) of Th(IV) decreases below 50% which indicates the good adsorption performance of *H. persicum* leaves in succeeding operating sorption cycles.

Table 6  
Comparison of Th(IV) sorption capacity of *Haloxylon persicum* leaves with other adsorbents

Adsorbent	pH	Adsorption capacity $q_e$ (mg/g)	Ref.
Cellulose composite	4.5	21.3	[2]
Perlite	5	5.8	[6]
Modified powdered waste sludge	5	27	[10]
Magnetic talc titanium oxide composite	5	56.6	[22]
Water hyacinth roots	4	20	[23]
Natural sepiolite	5	49.9	[25]
Polyvinylpyrrolidone magnetic activated carbon	3.5	149.35	[29]
<i>Haloxylon persicum</i> leaves	5	18.82	Present study

Table 6 shows the comparison of the absorption capacity of *Haloxylon persicum* leaves and other adsorbents from aqueous solutions. The data indicated that *H. persicum* leaves have an acceptable adsorption efficacy which shows the economic feasibility of using *H. persicum* leaves on a full-scale.

#### 4. Conclusion

The results confirmed that the *H. persicum* leaves, an available low-cost solid biomass, can be utilized for the effective removal of Th(IV) from aqueous systems. The sorption time reached the equilibrium at 60 min. Temperature (30°C–45°C) had a negative influence (exothermic behavior) on the sorption rate. The maximum removal percent (99.78%) and sorption capacity (18.82 mg/g) were obtained at pH 5, 40 mg/L Th(IV), 0.3 g dose, and 30°C. The isotherm and kinetic modeling indicate that the sorption data has well-fitting with the Langmuir and pseudo-second-order models owing to the higher correlation coefficient ( $R^2$ ) and lower chi-square analysis ( $\chi^2$ ) and MPSD than other models. The recycling study indicates the good sorption performance of *H. persicum* leaves in succeeding operating sorption cycles up to up to 7 cycles. Also, from the optimum sorption data and the best fitting isotherm, the sorption system can be scaled up to design a full-scale sorption system.

#### References

- [1] R. Pravalie, G. Bandoc, Nuclear energy: between global electricity demand, worldwide decarbonisation imperativeness, and planetary environmental implications, *J. Environ. Manage.*, 209 (2018) 81–92.
- [2] P.D. Bhalara, D. Punetha, K. Balasubramanian, Kinetic and isotherm analysis for selective thorium(IV) retrieval from aqueous environment using eco-friendly cellulose composite, *J. Environ. Sci. Technol.*, 12 (2015) 3095–3106.
- [3] M.A. Mahmoud, Adsorption of U(VI) ions from aqueous solution using silicon dioxide nanopowder, *J. Saudi Chem. Soc.*, 22 (2018) 229–238.
- [4] Y.M. Khawassek, A.M. Masoud, M.H. Taha, A.E.M. Hussein, Kinetics and thermodynamics of uranium ion adsorption from waste solution using Amberjet 1200 H as cation exchanger, *J. Radioanal. Nucl. Chem.*, 31 (2018) 493–502.
- [5] T.A. Saleh, M.T. Naemullah, A. Sari, Polyethylenimine modified activated carbon as novel magnetic adsorbent for the removal of uranium from aqueous solution, *Chem. Eng. Res. Des.*, 117 (2017) 218–227.
- [6] Z. Talip, M. Eral, U. Hicsonmez, Adsorption of thorium from aqueous solutions by perlite, *J. Environ. Radioact.*, 100 (2009) 139–143.
- [7] R.P. Han, W.H. Zou, Y. Wang, L. Zhu, Removal of uranium(VI) from aqueous solutions by manganese oxide coated zeolite: discussion of adsorption isotherms and pH effect, *J. Environ. Radioact.*, 93 (2007) 127–133.
- [8] M.A. Mahmoud, Kinetics and thermodynamics of U(VI) ions from aqueous solution using oxide nanopowder, *Process Saf. Environ. Prot.*, 102 (2016) 44–53.
- [9] A. Abutaleb, A.M. Tayeb, M.A. Mahmoud, A.M. Daher, O.A. Desouky, O.Y. Bakather, R. Farouq, Removal and recovery of U(VI) from aqueous effluents by flax fiber: adsorption, desorption and batch adsorber proposal, *J. Adv. Res.*, 22 (2020) 153–162.
- [10] M.Y. Pamukoglu, B. Kirkan, M. Senyurt, Removal of thorium(IV) from aqueous solution by biosorption onto modified powdered waste sludge: experimental design approach, *J. Radioanal. Nucl. Chem.*, 314 (2017) 343–352.
- [11] M.O. Abd El-Magied, A.A. Tolba, H.S. El-Gendy, S.A. Zaki, A.A. Ati, Studies on the recovery of Th(IV) ions from nitric acid solutions using amino-magnetic glycidyl methacrylate resins and application to granite leach liquors, *Hydrometallurgy*, 1 (2017) 89–98.
- [12] R. Kumar, S.A. Ansari, P. Kandwal, P.K. Mohapatra, Pertraction of U(VI) through liquid membranes using monoamides as carrier ligands: experimental and theoretical studies, *J. Radioanal. Nucl. Chem.*, 323 (2020) 983–991.
- [13] L. Dolatyari, M.R. Yaftian, S. Rostamnia, Multivariate optimization of a functionalized SBA-15 mesoporous based solid phase extraction for U(VI) determination in water samples, *Anal. Sci.*, 33 (2017) 769–776.
- [14] M.J. Kang, B.E. Han, P.S. Hahn, Precipitation and adsorption of uranium(VI) under various aqueous conditions, *Environ. Eng. Res.*, 7 (2002) 149–157.
- [15] L. Dolatyari, M. Shateri, M.R. Yaftian, S. Rostamnia, Unmodified SBA-15 adsorbents for the removal-separation of Th(IV) and U(VI) ions; the role of pores channels and surface active sites, *Sep. Sci. Technol.*, 54 (2019) 2863–2878.
- [16] L. Dolatyari, M.R. Yaftian, S. Rostamnia, Adsorption of Th(IV) and U(VI) on functionalized SBA-15 mesoporous silica materials using fixed bed column method; breakthrough curves prediction and modeling, *Sep. Sci. Technol.*, 53 (2018) 1282–1294.
- [17] L. Dolatyari, M.R. Yaftian, S. Rostamnia, Th(IV)/U(VI) sorption on modified SBA-15 mesoporous materials in fixed-bed column, *Iran. J. Chem. Chem. Eng.*, 36 (2017) 115–125.
- [18] L. Dolatyari, M.R. Yaftian, S. Rostamnia, Removal of uranium(VI) ions from aqueous solutions using Schiff base functionalized SBA-15 mesoporous silica materials, *J. Environ. Manage.*, 169 (2016) 8–17.
- [19] V.E.A. Post, S.I. Vassolo, C. Tiberghien, D. Baranyikwa, D. Miburo, Weathering and evaporation controls on dissolved uranium concentrations in groundwater—a case study from northern Burundi, *Sci. Total Environ.*, 607 (2017) 281–293.

- [20] M.A. Mahmoud, Removal of uranium(VI) from aqueous solution using low cost and eco-friendly adsorbents, *J. Chem. Eng. Process Technol.*, 4 (2013) 169, doi: 10.4172/2157-7048.1000169.
- [21] M.O. Abd El-Magied, A. Mansour, F.A. Alsayed, M.S. Atrees, S.A. Eldayem, Biosorption of beryllium from aqueous solutions onto modified chitosan resin: equilibrium, kinetic and thermodynamic study, *J. Dispersion Sci. Technol.*, 39 (2018) 1597–1605.
- [22] A.M.A. Morsy, Performance of magnetic talc titanium oxide composite for thorium ions adsorption from acidic solution, *Environ. Technol. Innovation*, 8 (2017) 399–410.
- [23] A. Ashraf, A.A. Hany, S. Shawky, A.T. Kandil, Separation of thorium from aqueous solution by non living water hyacinth roots, *Tech. J. Eng. Appl. Sci.*, 4 (2014) 1–9.
- [24] A.F.T.E. Din, E.A. Elshehy, M.O.A.E. Magied, A.A. Atia, M.E. El-Khouly, Decontamination of radioactive cesium ions using ordered mesoporous monetite, *RSC Adv.*, 8 (2018) 19041–19050.
- [25] E.K. Esen, R. Donat, Removal of thorium(IV) from aqueous solutions by natural sepiolite, *Radiochim. Acta*, 105 (2017) 187–196.
- [26] Z. Dousti, L. Dolatyari, M.R. Yaftian, S. Rostamnia, Adsorption of Eu(III), Th(IV) and U(VI) by mesoporous solid materials bearing sulfonic acid and sulfamic acid functionalities, *Sep. Sci. Technol.*, 54 (2019) 2606–2624.
- [27] L. Dolatyari, M.R. Yaftian, S. Rostamnia, Adsorption characteristics of Eu(III) and Th(IV) ions onto modified mesoporous silica SBA-15 materials, *J. Taiwan Inst. Chem. Eng.*, 60 (2016) 174–184.
- [28] Y. Wu, D. Chen, L. Kong, D.C. Tsang, M. Su, Rapid and effective removal of uranium(VI) from aqueous solution by facile synthesized hierarchical hollow hydroxyapatite microspheres, *J. Hazard. Mater.*, 371 (2019) 397–405.
- [29] M.A. Mahmoud, A. Abutaleb, I.M. Maafa, I.Y. Qudsieh, E.A. Elshehy, Synthesis of polyvinylpyrrolidone magnetic activated carbon for removal of Th(IV) from aqueous solution, *Environ. Nanotechnol. Monit. Manage.*, 11 (2019) 100191, doi: 10.1016/j.enmm.2018.10.006.
- [30] O.Y. Bakather, N. Zouli, A. Abutaleb, M.A. Mahmoud, A. Daher, M. Hassan, M.A. Eldoma, S.O. Alaswed, A.A. Fowad, Uranium(VI) ions uptake from liquid wastes by *Solanum incanum* leaves: biosorption, desorption and recovery, *Alexandria Eng. J.*, 59 (2020) 1495–1504.
- [31] M.A. Mahmoud, Kinetics studies of uranium sorption by powdered corn cob in batch and fixed bed system, *J. Adv. Res.*, 7 (2016) 79–87.
- [32] M.A. Mahmoud, Separation of U(VI) ions from the aqueous phase onto polyphenol silica nanocomposite in the batch adsorption system, *Alexandria Eng. J.*, 60 (2021) 3819–3827.
- [33] M.A. Mahmoud, Preparation of magnetic nanomaterial for U(VI) uptake from the aqueous solution, *J. Saudi Chem. Soc.*, 25 (2021) 101214, doi: 10.1016/j.jscs.2021.101214.
- [34] M.A. Mahmoud, Design of batch process for preconcentration and recovery of U(VI) from liquid waste by powdered corn cobs, *J. Environ. Chem. Eng.*, 3 (2015) 2136–2144.